Eurographics Workshop on Visual Computing for Biology and Medicine (2018)
A. Puig Puig, T. Schultz, and A. Vilanova (Editors)

Visual Analysis of Regional Anomalies in Myocardial Motion

A. Sheharyar[1,2], A. Ruh[3], M. Aristova[3], M. Scott[3], K. Jarvis[3], M. Elbaz[3], R. Dolan[3], S. Schnell[3], K. Lin[3], J. Carr[3], M. Markl[3], O. Bouhali[2], and L. Linsen[1]

[1] Westfälische Wilhelms-Universität Münster, Germany
[2] Texas A&M University at Qatar, Qatar
[3] Feinberg School of Medicine, Northwestern University, Chicago, IL, USA

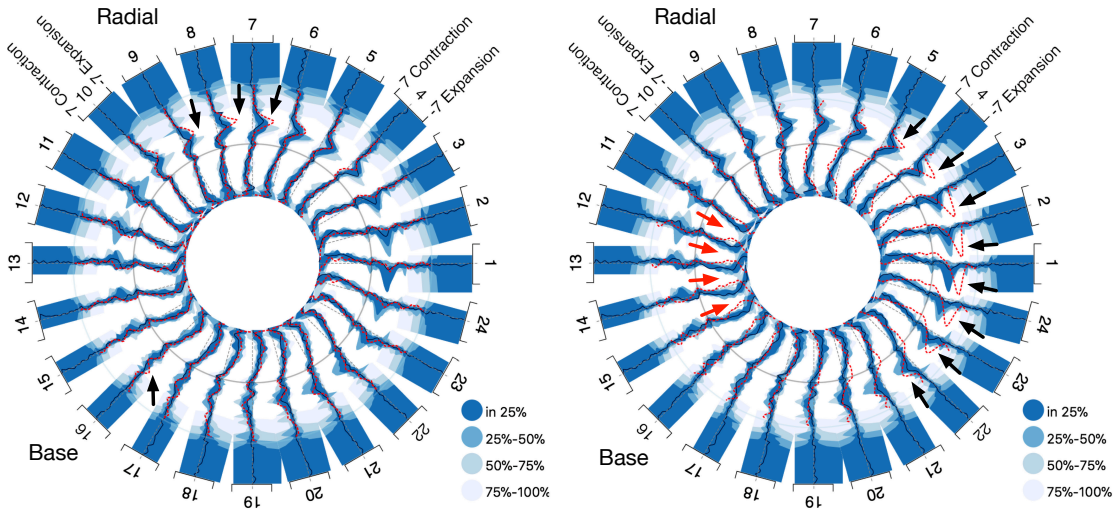

Figure 1: *Radial FBP for visual comparison of a healthy volunteer (left) and patient (right) datasets to a healthy volunteer cohort.*

Abstract

Regional anomalies in the myocardial motion of the left ventricle (LV) are important biomarkers for several cardiac diseases. Myocardial motion can be captured using a velocity-encoded magnetic resonance imaging method called tissue phase mapping (TPM). The acquired data are pre-processed and represented as regional velocities in cylindrical coordinates at three short-axis slices of the left ventricle over one cardiac cycle. We use a spatio-temporal visualization based on a radial layout where the myocardial regions are laid out in an angular pattern similar to the American Heart Association (AHA) model and the temporal dimension increases with increasing radius. To detect anomalies, we compare patient data against the myocardial motion of a cohort of healthy volunteers. For the healthy volunteer cohort, we compute nested envelopes of central regions for the time series of each region and each of the three velocity directions based on the concept of functional boxplots. A quantitative depiction of deviations from the spatio-temporal pattern of healthy heart motion allows for quick detection of regions of interests, which can then be analyzed in more detail by looking at the actual time series. We evaluated our approach in a qualitative user study with imaging and medical experts. The participants appreciated the proposed encoding and considered it a substantial improvement over the current methods.

1. Introduction

Abnormal function of the left ventricle (LV) increases the risk for cardiovascular complications and death after cardiac and non-cardiac surgery [DAS*14]. The evaluation of LV performance improves the risk assessment. Thus, an early detection of its dysfunction, monitoring, and accurate diagnosis is of great importance [FJS*09, MRG*13]. The LV function is often assessed using global indicators such as ejection fraction, ventricular volume, or stroke volume. However, these global indicators lack information about the local or regional ventricular function that can provide important biomarkers for several cardiac diseases and plays a crucial role in their diagnosis [FJS*09, MRG*13]. For instance, despite having normal ejection fraction, nearly 50% of the heart failure patients have anomalies in the diastolic function [WN09]. Therefore, in a thorough clinical analysis, regional wall motion anomaly analysis shall be preferred.

DOI: 10.2312/vcbm.20181239

Myocardial motion can be captured using a velocity-encoded magnetic resonance imaging (MRI) method called tissue phase mapping (TPM) [PSY*94], see Section 3. It allows for the evaluation of the heart's anatomy, the function of its chambers and valves, and the blood flow through major vessels (among other aspects) in a non-invasive manner with high spatial and temporal resolution [JFB*06]. TPM enables the extraction of myocardial velocities in all three spatial dimensions, which are transformed to radial, circumferential and longitudinal components with respect to the LV geometry, see Section 3. Due to the three-dimensional nature of the TPM, it is particularly well suited to study the complex motion of the LV in order to analyze the regional heart function [FJS*09].

In clinical practice, regional wall motion is often analyzed using a standard developed by the American Heart Association (AHA) [Cer02], which represents the LV with 17 standardized segments obtained from three short-axis slices. Such analysis relies on visual assessment and interpretation of the motions of each segment. This interpretation is time-consuming and highly dependent on the experience of the clinician and, thus, has high inter-observer variability [RKL*07]. There has been a significant research effort in automated anomaly detection in the wall motion [PBI*13,SFK*09] to reduce the subjectivity of the assessment. However, there is little attention paid to developing improved visualization tools for the assessment. The goal of this paper is to present a novel approach for the visual assessment of regional wall motion anomalies to assist clinical researchers.

Our approach is based on a radial layout similar to the AHA model that cardiologists are familiar with. We lay out the segments in the same manner to capture the spatial distribution within each of the three slices. To encode the temporal dimension we use the radius of the radial layout, thus, allowing for the analysis of spatio-temporal patterns [SCK*16]. We use the concept of functional box plots (FBPs) for the time series of each segment and each velocity dimension to capture the variability within the healthy cohort, and to visually encode spatio-temporal regions of anomalies. We document the effectiveness of our approach using patient and healthy volunteer datasets, see Section 5. Our approach is evaluated in Section 6 by conducting qualitative user studies with imaging and medical experts.

2. Related Work

To our knowledge, visual assessment of regional anomalies in myocardial motion has not been fully addressed in the literature. The focus of the academic community has been more towards the automatic detection of anomalies [PBI*13, SFK*09], which by itself does not facilitate an intuitive understanding of the spatio-temporal behavior. Most of the studies use the 17-segment model developed by the American Heart Association (AHA) [Cer02]. This model is the most common way of showing the myocardial motion. For instance, Barnes et al. [GBGCP08] use the AHA-based bullseye charts to highlight abnormal regions in pathological cases. Punithakumar et al. [PBI*13] worked on automatic detection of regional anomalies and demonstrated the results of their algorithm on a color-coded AHA-based plot. The major limitation of all approaches using the exact AHA model is that it shows the data for a single time step only. Several individual AHA plots are then needed to investigate the temporal behavior throughout the cardiac cycle. Our visualizations are based on a spatio-temporal layout that allows for the analysis of the spatio-temporal behavior of anomalies.

A somewhat smaller limitation of the AHA model is that it represents the myocardium with very few regional segments only. A higher spatial resolution would be desirable for a more fine-grain analysis of regional myocardial motion. Föll et al. [FJS*09] used an extended version of the AHA model with 24 segments for each of the three short-axis slices. They encode average myocardial velocities of normal volunteers of various age groups and perform a correlation analysis with the data of a patient with dilated cardiomyopathy to find the differences in regional LV dynamics for all three velocity components. However, the correlation analysis does also not provide any temporal information of the correlation results. Based on discussions with medical experts, we follow the idea of Föll et al. to use a higher spatial resolution, but enhance it to a spatio-temporal layout.

A recent study by Codreanu et al. [CPS*15] for assessing LV wall motion anomalies using TPM imaging compares the anomalies in the patients having coronary artery disease with a group of healthy volunteers. They generated graphs of velocities over time and arranged them radially next to the corresponding segments for each slice and each velocity direction separately. For representing the velocities for the cohort of healthy volunteers they merely showed the average, which does not allow for an understanding of how much variation exists within the group. Our approach, instead, is based on the concept of functional boxplots, which allows for the assessment of the variation within the healthy group and the visual comparison of a patient dataset against that group.

Clarysse et al. [CHCM02] performed a functional data analysis on the spatio-temporal deformation of the myocardium during systole from tagged MRI. To visualize the MR data of six short-axis slices with 12 segments each, they used a polar plot to study the spatial deformation at a single time step and, in a separate representation, a rather large matrix of 6×12 small multiples to investigate the temporal patterns. They highlighted the abnormal regions with dashed lines. In this matrix of views, it is quite challenging to correlate the temporal patterns among different segments to their spatial distribution in the polar plot. Also, the anomalies are not quantified and not temporally located, i.e., it is not clear how much the velocities deviate from a normal behavior and in which part of the cardiac cycle. The visual encodings we propose allow for such an analysis.

Taimur and Hua [TH13] proposed a 3D model-based approach to study the dynamic object deformations such as cardiac motion. They developed a classification and visualization method based on the medial surface shape space, in which two shape descriptors were defined for differentiating normal and abnormal human heart deformations. The 3D visualizations are inherently difficult to comprehend due to occlusion issues. Our approach, instead, is based on the 2D design that is easier to analyze.

Our paper is based on the spatio-temporal visualization of regional myocardial velocities presented in our earlier work [SCK*16]. The main approach is given in Section 3.3. However, in our previous work, we were only visualizing the motion of individual datasets. The goal of this paper is to show anomalies by vi-

sualizing cohorts of healthy volunteer data and visually comparing a patient dataset to this cohort to observe if abnormal behavior is present (pathological case), where it happens (spatial dimensions), when it happens (temporal dimension), and how severe it is (quantified deviation).

3. Prerequisites and Problem Description

3.1. Image Data Acquisition

TPM imaging for LV myocardial motion has proven to be a robust technique offering high spatial ($< 2mm$) and temporal ($\approx 20ms$) resolution when compared to other acquisition techniques [CHS*16] such as tagging [ZPR*88]. For the healthy cohort, we have used the data acquired for the reproducibility study performed by Lin et al. [LCB*16]. In that study, 19 healthy subjects (13 men, 6 women, age $= 49.94 \pm 15.43$ years) with normal cardiac function and no history of cardiovascular disease were scanned. Each subject underwent two separate MRI scans, using the same imaging method with a time difference of 16.63 ± 6.58 days between the two scans. This makes a total of 38 healthy datasets.

Three short-axis image slices (base, mid-ventricular, and apex) along the LV were acquired according to the recommendations by the AHA, as shown in Figure 2. For each slice, a magnitude and three velocity-encoded images (one for each of the three spatial dimensions in an image-aligned 3D Cartesian coordinate system) are acquired. All scans were performed on a routine 1.5T MRI system (Magnetom, Aera, Siemens, Germany) using a black-blood prepared 2D gradient echo (GRE) cine phase-contrast MRI sequence with three-directional myocardial velocity encoding [JFB*06, MRG*13]. Other imaging parameters included: spatial resolution=$1.98 - 2.29 \times 1.98 - 2.29$ mm^2, slice thickness=8 mm, and temporal resolution=$20.4 - 20.8$ ms/frame.

Three patient datasets (P_1 to P_3), all diagnosed with dilated cardiomyopathy, were acquired using the Siemens Avanto 1.5T MRI machine with imaging parameters as spatial resolution=$2.1875 - 2.25 \times 2.1875 - 2.25$ mm^2, slice thickness=8 mm, and temporal resolution=$22.8 - 24.4$ ms/frame. P_1, a 52 years old male, has 40% ejection fraction ($< 50\%$ is considered bad) and is known to have abnormalities primarily in the radial direction in the septum in all slices. P_2, a 67 years old female, has significant inflammation with 60% ejection fraction and P_3, also a 67 years old female, has little inflammation with 52% ejection fraction.

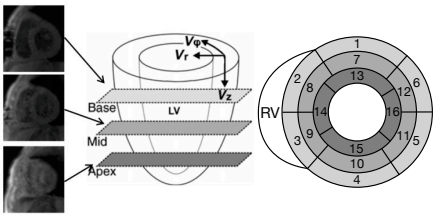

Figure 2: *Acquisition of basal, mid, and apical slices. [CNS*15]*

3.2. Data Processing and Preparation

The healthy datasets were processed using an in-house software developed in MATLAB. The epicardial and endocardial LV contours were manually traced in all three slices for all acquired cardiac time frames to segment the LV. However, the patient datasets were segmented using a semi-automatic segmentation technique based on contour propagation and particle tracing [CHS*16]. The segmentation step results in a binary mask of the myocardium for each time step, which is partitioned into 24 segments to get a higher spatial sampling. The velocities are converted to a cylindrical coordinate system that is aligned with the LV and consequently represents radial, circumferential, and longitudinal velocity components of the myocardium (see Figure 2). This mask and partition is applied to all velocity-encoded images to extract the regional velocity information. Velocities within each segment are averaged to compensate for noise.

For all of the acquired datasets, imaging started at the beginning of the systolic phase (acquisition is ECG-gated to the R-wave), but not the full cardiac cycle was measured for all subjects. The used prospective gating needs dead time (10-20%) at the end of the cardiac cycle to be able to catch the next trigger signal. In order to have comparable spatio-temporal patterns, the individual datasets need to be synchronized, which was rather challenging due to incomplete cycles and missing heart rates. The only point in time (except the starting point) that can be detected sufficiently reliable in all datasets was the end-systolic point (ES) when the heart transitions from the systolic to the diastolic phase. The ES is the point in time within the cardiac cycle with minimum LV area. We compute the LV area by counting the number of pixels inside the myocardium within the given slice. We split all time series at the ES into a systolic and a diastolic phase. Then, the systolic phases have a well-defined starting and end point and can be synchronized using linear time interpolation [JFB*06]. Independently, the diastolic phases are interpolated, but due to the different ending times they only have a synchronized starting point. Figure 3 shows the radial velocities (averaged over all segments) in the mid-ventricular slice after synchronization. The different end points of the time series are apparent.

After these data preparation steps, we obtain for each dataset an unsteady 3D vector field, where spatial sampling is provided within a region of interest (LV myocardium) on three distinct 2D image slices (apex, mid-ventricular, and base) and aggregated over 24 segments per slice. The 3D vectors are given with respect to a cylindrical coordinate system. The evolution of the 3D vector field is measured over a maximum of 100 time steps from one (incomplete) cardiac cycle, which are synchronized at beginning and end of the systolic phase.

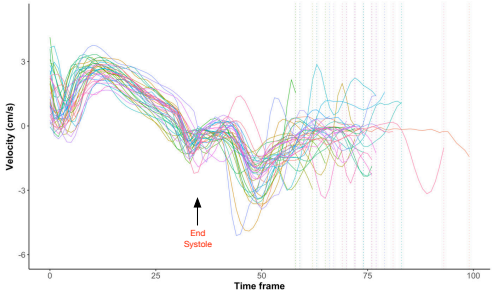

Figure 3: *Averaged radial velocities of mid-ventricular slice for all datasets from healthy volunteer cohort.*

3.3. Radial Layout for Spatio-temporal Visual Analysis

In our previous work, we proposed a spatio-temporal layout for visualizing regional myocardial velocities for individual datasets [SCK*16]. In this paper, we want to build upon this layout to visualize cohorts and differences of individual datasets when compared to cohorts (anomalies). The spatio-temporal layout amends the idea of the AHA model to radially lay out the segments. Hence, spatial information is encoded by the angular coordinate (azimuth) in the radial layout (polar coordinates). We use a finer spatial granularity than the AHA model with 24 segments per slice. The temporal dimension is then mapped to the radial coordinate in the layout, where the time series does not start in the center but at a larger radius to avoid visual clutter towards the center. In this radial layout, we can depict velocities using various encodings (cf. [SCK*16, TBB*08]), for example, by a color mapping of the velocities, see Figure 4. In Figure 4 (left), we created one radial plot for each of the three slices and each of the three velocity components leading to a visualization with 3×3 views. This image encodes the entire spatio-temporal information of a single dataset. Hence, one still image can replace going sequentially through all images of all velocity components and all time steps. The continuous color mapping uses blue color for negative and red color for positive values, where values close to zero can be shown in white or transparent. We also highlight beginning and end of the systole and diastole phase and label the AHA segments. Since medical experts are most familiar with the AHA plots, an AHA-based visualization of a single, interactively selected time step is also supported in the interactive visual analysis tool, see Figure 4 (right column).

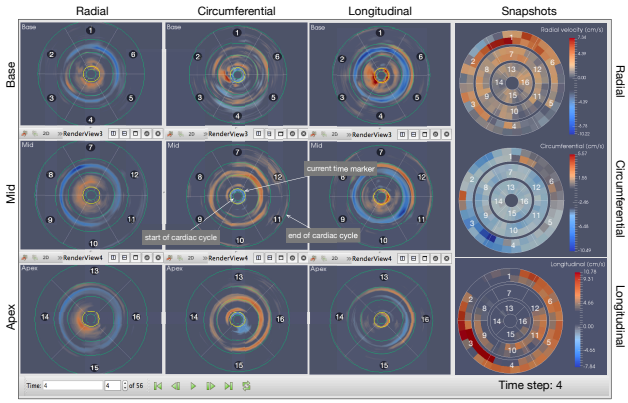

Figure 4: *Linked views of 3×3 spatio-temporal views of individual slices (rows) and velocities (left three columns) and spatial views of selected time step (right column). [SCK*16]*

3.4. Anomaly Analysis Tasks

Anomaly analysis refers to the process of finding patterns or values which do not conform to the patterns or values of some reference data. Within the medical context the reference data are typically provided in the form of a selection of datasets from healthy people (commonly volunteers). In the case of spatio-temporal patterns, locations in space and time of anomalies are of interest. Moreover, one would also like to know how severe an anomaly is, i.e., how much it deviates from the normal state. These objectives also hold true for our application scenario and can be summarized as:

T1 *Visualize variability within a cohort*. The goal is to observe the variability in the patterns within a cohort of healthy volunteers. In order to be able to judge anomalies, one needs to know how much variation is normal.

T2 *Visually compare individual datasets to a cohort*. The goal is to analyze whether a patient dataset matches the spatio-temporal pattern of the cohort of healthy volunteers.

T3 *Visually encode location of anomalies*.The goal is to see where an individual dataset in the case of pathology deviates from the spatio-temporal pattern of the cohort of healthy volunteers. Of interest are both the spatial location (segment) and the time point (phase) of the anomaly.

T4 *Visually encode severeness of anomalies*.The goal is to quantify how much an individual dataset in the case of pathology deviates from the spatio-temporal pattern of the cohort of healthy volunteers.

4. Visual Encodings

Starting from the analysis tasks described in the previous section, we developed visual encodings suitable for fulfilling the respective tasks. The visual encodings address different aspects of a visual analysis of anomalies in the spatio-temporal patterns of regional myocardial motion captured by TPM imaging for individual patients in comparison to a reference cohort of healthy volunteers. We present the visual encodings with increasing task complexity (T1 - T4) in Sections 4.1-4.4, while the analytical workflow would make use of the visual encodings in reverse order, i.e., starting from an overview and providing more details on demand, see Section 4.5.

4.1. Functional Box Plots (FBPs)

Our first goal (Task T1) is to visualize the variability within a cohort. Variability of a numerical attribute is often captured and visualized using boxplots. They cover median, interquartile range, upper and lower quartiles, and outliers of the statistical distribution. For each member of a cohort we have a time series of velocity values, i.e., the velocity is a function of time. When dealing with functions rather than values, the concept of functional box plots (FBP) [SG11, HS10] has been introduced. They are based on the concept of band depth, which allows for ordering functional data from the center outwards, i.e., according to decreasing depth values. The median area is then the band with the highest depth and the central 50% of the curves is the analog to the interquartile range. Lui et al. [LPS*99] introduced the concept of central regions, where a central region envelopes a proportion of deepest curves from the sample. We follow this concept and define four central regions covering 25%, 50%, 75%, and 100% of the functions, see Figure 5a. We apply a single-hue luminance color map for encoding the sequence of four central regions (all color maps within this paper were generated using ColorBrewer [HB03]). The FBP conveys better the shape of the time series when compared to the standard boxplots applied to each time point, cf. [SG11].

The FBP requires all time series to be of equal length, which is

not the case in our datasets. Thus, we divide the temporal dimension into five intervals where 100%, 75%, 50%, 25%, or at least one of the time series are present, see Figure 5a. Then, we can compute the FBP for each of the five intervals separately (for all time series that exist throughout the interval) and stitch them together. The plots exhibit discontinuities at the stitches, which is desired to visually reveal the five intervals. For the visual encoding of the results, we should take into account that having less data increases the uncertainty, i.e., the bands should widen when some time series stop. We achieve this by setting the values of the missing time series for each interval to the minimal and maximal observed diastolic values.

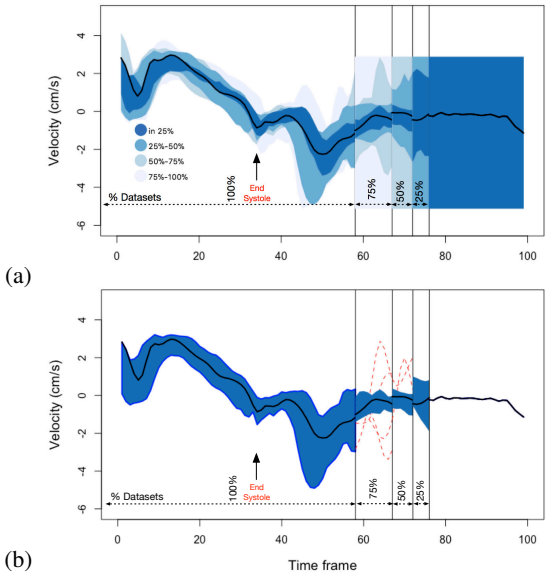

Figure 5: *Functional box plot (a) and outlier detection (b).*

4.2. Radial FBPs

When applying FBPs to a cohort, we get four central regions for each LV segment of each slice (base, mid, and apex) and each velocity direction (radial, circumferential, and longitudinal). To allow for an understanding of spatio-temporal patterns of the variability within a cohort, we have to use an intuitive layout of all these FBPs. We adopt the radial layout concept described in Section 3.3, which was shown to be effective for analyzing spatio-temporal patterns in myocardial motion [SCK*16]. Figure 6 demonstrates the design methodology of the layout. The FBPs for all segments are arranged along the angular direction (same as in Section 3.3) to capture the spatial structure of the LV. The temporal dimension is mapped to the radial coordinate, i.e., time increases with increasing distance from the center. The display space for each FBP is a rectangle, though, and not a trapezoid to avoid any distortions, i.e., the function values at the beginning and at the end of the time series remain comparable. All FBPs are normalized to the global minimum-maximum range and the plots are scaled accordingly to fit the display space. The visualizations are also enhanced by marking the cardiac phases as rings, and the velocity directions are labeled, e.g., as contraction or expansion for radial velocities (not shown in the sketch in Figure 6). We refer to this radial layout of FBPs according to the spatio-temporal dimensions as *radial FBP*.

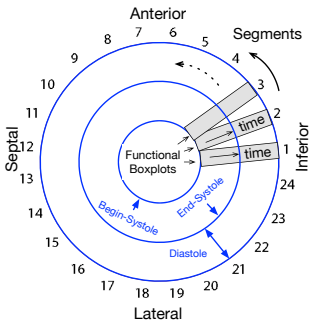

Figure 6: *Design idea for layout of radial FBP.*

For the anomaly analysis, we want to convey whether an individual dataset matches the spatio-temporal pattern of the cohort of healthy volunteers (Task T2). We overlay the radial FBPs with the velocity values of the individual dataset for all FBPs in the layout, see Fig. 1. The time series of the individual dataset is shown in red. One can observe whether the red curve follows the pattern of the four nested bands. Note that Fig. 1 shows the anomalies for the radial velocity in the base slice only. To analyze the complete dataset for all three velocities and all three slices, we would have to investigate 3×3 such images, cf. Figure 4 or Figure 9.

4.3. Highlighting Anomaly Regions

The goal of analysis Task T3 was to show where an individual dataset deviates from the cohort. This can be observed in our radial FBPs, as they contain all information. However, differences may be subtle and when looking at the overview of 3×3 radial FBPs, the display area of each radial FBP is limited. Thus, when starting the visual analysis with an overview of all velocity directions in all slices, a less detailed encoding that highlights where deviations occur is desirable. Consequently, we propose to highlight the segments (regions) in the radial FBPs where the time series of the patient dataset is significantly different from the cohort.

To test for significance in the difference, we add the patient dataset to the cohort and test, whether it is an outlier in the FBP. In the construction of the FBP, observations (functions) are ordered by a notion of band depth that allows ordering the functions from the center outwards and thus provides a measure to define functional quartiles and the centrality or outlyingness of an observation [SG11]. The outliers in the FBP can be detected by considering an envelope of 1.5 times the 50% central region. This is motivated by the empirical rule of taking 1.5 of the interquartile range for detecting outliers in conventional boxplots. Thus, for FBP, fences are obtained by inflating the envelope of the 50% central region to 1.5 times its width [SG11]. Any observations outside the fences are marked as potential outliers. Figure 5b shows the envelope for outlier detection in an FBP. Outliers are shown in red. The outliers are computed for each interval separately. For highlighting outliers, we only detect them in the time interval, where 100% of the time series are available, as this is the most important and most reliable part.

Figure 7 shows a radial FBP for comparing patient data against a healthy cohort with those time series, where the patient is detected to be an outlier marked with a red dot and a red color for the segment number. The markers directly attract the attention towards the respective segments.

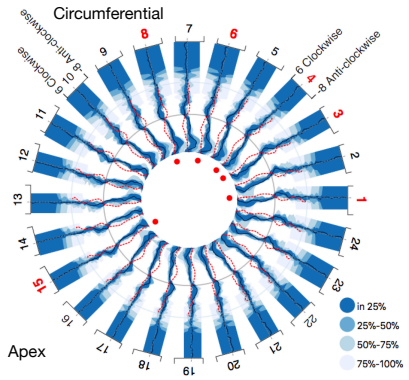

Figure 7: *Outliers (red dots and numbers) in radial FBP for circumferential velocities in the apical slice of patient P_1 (Task T3).*

4.4. Difference-encoded Radial FBPs

The outliers in the radial FBPs show effectively where the regions of abnormal motions are, but they do not encode how severe these anomalies are, e.g., how far the velocity values lie outside the 100% band and whether the values are too low or too high when compared to the cohort. Moreover, the outlier highlighting marks entire segments, but not the time frames within the respective time series when the deviations occur. These aspects, though, are captured in the radial FBP. The radial FBP encodes the actual velocity values for the cohort in comparison to the velocity values for the individual dataset that we test against the cohort. If we want to quantify their differences (Task 4), then we can derive this information from the radial FBP, but it may be more effective to explicitly encode the differences. We propose to display such differences (the amount of anomaly) by amending the radial FBP.

Amending the radial FBP allows for encoding the differences to all central regions in one plot. We plot the difference from each of the central regions in a nested fashion. To not confuse these plots with the radial FBPs above, we use a different coloring scheme for the bands, namely another single-hue luminance color map for a different hue.

The difference is considered to be zero if a value lies between the minimum and maximum values of the region, otherwise, the difference is calculated from the minimum and maximum boundaries of the region. Figure 8b shows an example of displaying the difference in a radial FBP. The outer-most band shows the difference between the patient velocities to the 25% central region of the velocity-encoded FBP, next to the 50% region, then to the 75% region, and the inner-most band shows the difference to the 100% region. It can be observed with this encoding that the severeness of the anomaly can vary a lot for different potentially abnormal regions. The differences in the radial FBP also show the sign of the differences and not only the magnitude, i.e., it can be observed whether the velocities are too high or too low. The difference encoding can, of course, also be combined with the outlier highlighting, see Figure 8b.

4.5. Analytical Workflow

When starting to analyze a dataset, the user would first of all like to get an overview, i.e., the user would like to see the information about all time steps of all segments for all three slices and all three velocity directions. Hence, the user would start with a 3×3 radial FBP view. Since analyzing these data is rather complex and the visual complexity may be overwhelming, the user needs guidance, which we provide by starting with difference plots (enhanced with highlighted outliers) as in Figure 9. The difference plots and the outlier highlighting quickly guides the user to regions that are potentially interesting for further inspection.

How to proceed from here depends on the individual case. If one of the 3×3 plots exhibits strong differences, one may click at that plot and further analyze it, cf. Figure 8c. Within that radial FBP one may observe some segments that are of interest, which can then be clicked at to analyze an individual FBP, cf. Figure 5a. A second scenario would be that one segment exhibit strong difference in all 3×3 plots such that one would click immediately at that segment to analyze a 3×3 plot of that segment only. During the process of going from overview to detail, the user may at any time switch between the difference encoding and non-difference encoding, cf. Figure 7. The final analysis after providing detailed views is performed on the FBPs that show the actual time series and not on the difference encoding.

5. Results

To visually encode the variability in a cohort (Task T1), we produced functional box plots for each segment for the healthy cohort and arranged them in a radial layout (see Sections 4.1 and 4.2). For instance, Figure 10 shows the velocity values and their variability in the healthy cohort for the radial velocities in the basal slice. First of all, the radial FBP indicates the complex motion behavior of the myocardium, which also for healthy people does not simply compress and expand equally in all regions. Instead, the individual FBP exhibit some clearly different behaviors in different segments. This is because the heart is simultaneously shrinking/elongating and rotating. Moreover, we can see that the variation within the cohort also differs for different segments and different cardiac phases. In particular, we can observe that the healthy datasets have higher variability in the diastole phase for segments that have been marked with arrows of different colors. The black arrows indicate stronger radial motion in segments 1, 2, and 24 than other segments. Similarly, the red arrows indicate opposite directions between 50% and 75% regions at segments 11-12, and the orange arrows indicate higher velocities in the 50% central region than the 25% region in segments 21-23 in diastole. Such a visualization of cohorts can be helpful for training and teaching purposes of still inexperienced medical students or doctors. Note that Figure 10 shows just one velocity for a single slice. For a complete analysis, one would require a matrix of 3×3 views.

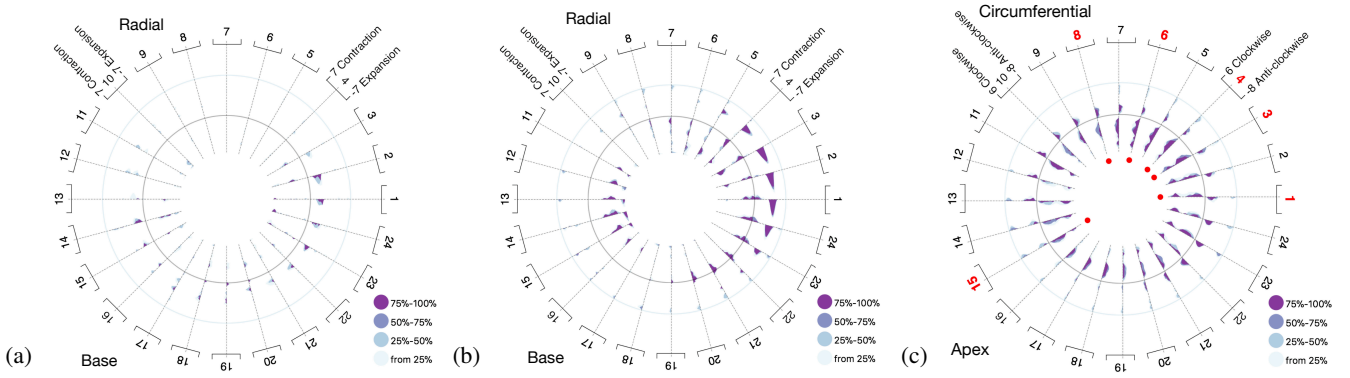

Figure 8: *Difference-encoded radial FBPs of (a) healthy volunteer vs (b) patient (Task T4) and (c) with outlier highlighting (Task 3).*

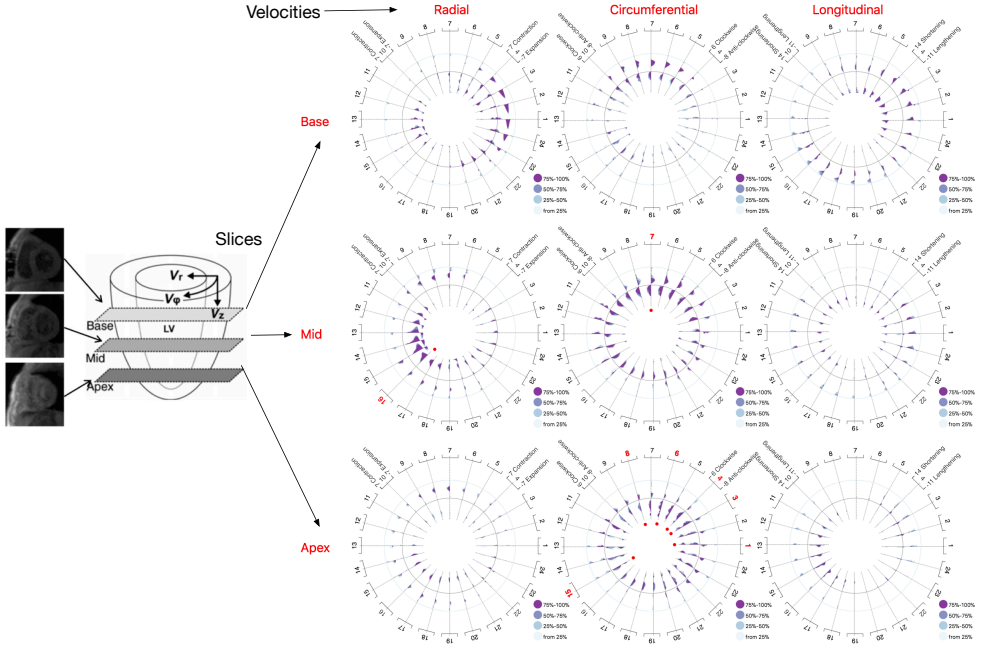

Figure 9: *Difference-encoded radial FBPs of a patient showing all slices and velocities with outlier highlighting (Tasks T3 and T4).*

For visual analysis of anomalies, we can show the velocities of an individual dataset (usually a patient) on top of the visual encoding of a cohort, to see if the individual dataset matches the spatio-temporal patterns of the cohort (Task T2). Figure 1 (left) shows the cohort with a healthy dataset H_1 overlaid as a red dotted line. The healthy dataset was one of the 19 volunteers mentioned above, where the reference model was then built by considering only the other 18 volunteers. We can observe that except for few segments that go out of the healthy range (100% central region) in the late diastole (marked with black arrows), the red line mainly stays within all central regions of all FBPs, i.e., the red line matches the bands quite well. On the other hand, the visualization of the pathological dataset P_1 in Fig. 1 (right) exhibits stronger deviations of the red line from the bands indicating anomalies. In particular, we observe anomalies on the septal side (left in the image) in the systole (marked with red arrows) and on the lateral side (right in the image) in the diastole (marked with black arrows). The red arrows indicate segments where there is a slight expansion (negative velocities) in the systolic phase in segments 12 to 15, where there should be no expansion, but contraction, as indicated by the bands having positive velocities. This anomaly is a clear indicator of a pathological case, possibly caused by a scar. The black arrows indicate a very strong expansion (negative velocities) in the diastole on the opposite side (segments 1 to 5 and 22 to 24). While there should be expansion in the respective phase at these segments, there is a clear overshooting of the red line. A possible explanation of this abnormal behavior is that the lateral side tries to compensate the anomaly on the septal side by expanding strongly in order to maintain a certain blood pressure. The observations confirm the initial diagnosis of the patient's condition.

The anomalies for the two other patients P_2 and P_3 that we investigated were less obvious than for patient P_1. In fact, for patient P_2 only the circumferential velocities in the apical slice showed obvious deviations from the healthy cohort in inferior lateral and

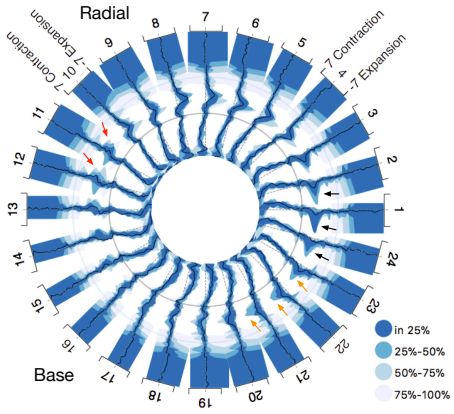

Figure 10: *Radial FBP to visualize cohort variability (Task T1).*

anterior regions, see black arrows in Figure 11a, while for patient P_3 only the radial velocities in the apical slice showed obvious deviations from the healthy cohort, see black arrows in Figure 11b.

Figure 7 shows the radial FBP of circumferential velocities in the apical slice with the statistical outliers marked in red color. This encoding combined with the patient (P_1) velocities on top of the visual encoding of a cohort was meant to serve for highlighting spatio-temporal regions of potentially abnormal behavior (Task T3). Hence, the outlier markers quickly pinpoint the spatio-temporal locations of abnormal areas. When looking at Figure 7, one can immediately see that segments 1, 3, 4, 6, 8, and 15 have been identified as outlier segments.

While the outliers in the radial FBP plot above only show regions of abnormal behavior, Task T4 was concerned with the quantification of the anomalies, see Section 4.4. Figure 8 shows the differences of the radial velocities in the basal slice to the cohort when using radial FBPs for healthy dataset H_1 and patient dataset P_1. We can now observe for which time frames differences occur and whether the velocity values are too high or too low. For example, for the patient dataset, in the systole we see that there is not enough contraction, while in the diastole there is too much expansion, indicating why this patient has a too low ejection fraction.

Finally, a 3×3 combined plots of outlier indicators (Task T3) and differences (Task 4) can be used to highlight the key areas of potential anomaly in all slices and velocity directions. Figure 9 shows an example patient P_1. One can observe that the radial velocities in the basal slice show greater differences in the right side of the myocardium while in mid slice, the differences are rather on the left side. One of the segments (16) has also been marked as a statistical outlier. (3×3 plots for all visual encodings are presented in full detail for both H_1 and P_1 in the supplementary material.)

6. Evaluation

We conducted a user study to qualitatively evaluate the effectiveness of our approach. Seven experts (4 imaging and 3 medical experts), familiar with the concept of TPM imaging, and having experience levels between 1 and 10 years, participated in the study. The study had two stages. In the first stage, in a roughly 30-40 minutes long session, participants were introduced to the project and got familiarized with the proposed visualization methods and analytical workflow. They were asked to give their general feedback on the intuitiveness and effectiveness of our visual encodings and were asked to rate the proposed visual encoding on a 5-step Likert scale (with 1 being worst and 5 being best) in terms of intuitiveness.

All participants appreciated the proposed encoding and considered it a substantial improvement over the commonly used AHA-based methods. They liked the idea of presenting a lot of data in a very compact format and also appreciated the use of a spatial layout as it matches that of the heart and makes areas of abnormal velocity patterns stand out. They liked the difference-encoded plots as a quick and faster way for screening the patterns of abnormality to reduce the user input and also the number of individual images that users must examine. They also appreciated the emphasis on the uncertainty of the measurements (using the five time intervals) in terms of presenting from how much of the normal volunteers data was inferred. In terms of intuitiveness, the average rating was 4.14 (out of 5). Some of the participants mentioned that initially they had difficulty understanding the bands and colors, but once they "got their head around it", it was actually intuitive. A couple of participants commented that the 3×3 view of all slices and velocity directions with 24 segments is a lot of information and one participant even proposed to consider using just 16 segments. Two of the participants (with more experience) suggested to include time-to-peak (TTP) and dyssynchrony calculations [FJG*11], which would be useful in clinical settings.

The second stage of the user study was a task in which participants were required to visually assess two healthy and two patient datasets (without knowledge of being healthy or patient and also different from the ones used in the first stage) and to explain how they analyze the data. Each dataset was presented with our tool and for comparison with AHA-based visualizations as shown in Figure 12, which reflect common practice. The first observation was that AHA model visualizations by themselves did not allow for a proper judgment whether there is a pathology. Participants with imaging background or less (or no) clinical experience asked for a reference or ground truth that they could use to compare with the given dataset. We then provided such a reference (see Figure 12) in the form of the average of the healthy volunteer cohort (without indicating variance), but it was still too difficult for them. Using our tool instead allowed the participants to detect spatio-temporal anomaly regions in patient data. On the other hand, some participants interpreted deviations of the time series from the bands for healthy people also as (mild) pathologies.

One medical expert mentioned that our visual encodings could be applied to any cardiovascular magnetic resonance imaging parameter, such as segmental strain analysis, perfusion, LGE, T2/T1/ECV, as long as one can acquire a good sample of healthy control values. Another participant mentioned that this tool might be integrated with the AHA representation in the sense that, once the users have identified a certain time step of a certain velocity direction as relevant, the respective AHA plot could be shown. We actually have this addition implemented, but did not include it into the user study to keep things separated and not elongate this study too much.

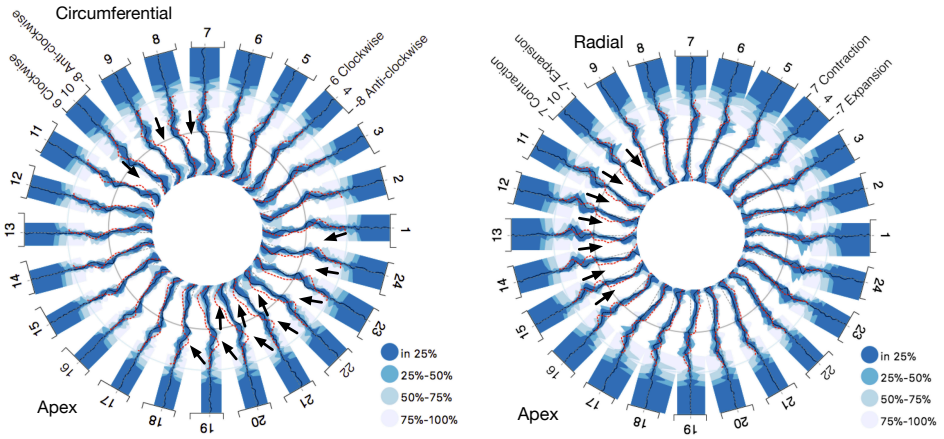

(a) *Circumferential velocities in apical slice (Patient P_2)* **(b)** *Radial velocities in apical slice (Patient P_3)*

Figure 11: *Radial FBP for visual comparison of patients P_2 (left) and P_3 (right) datasets to a cohort (Task T2).*

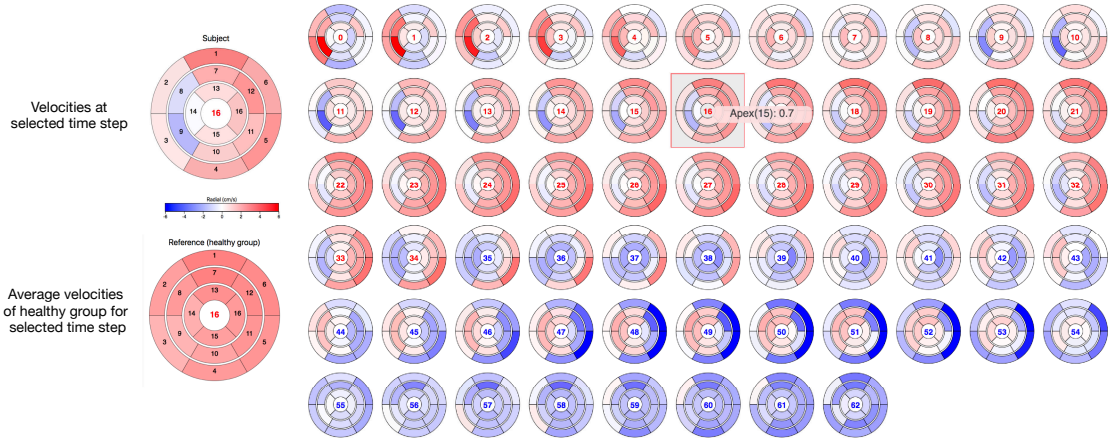

Figure 12: *Radial velocities in the basal slice of a patient (P_1) represented as the AHA model. The right side has a series of smaller plots, one for each time step of the patient data.*

7. Discussion and Future Work

It is important to point out that TPM is not yet clinical routine. Consequently, we do not have massive numbers of datasets yet and most medical experts have not yet dealt with analyzing such data. Having more datasets would help in forming a better healthy control cohort, to which we compare. In particular, we did not consider any demographics for our cohort. Currently, the cohort mixes volunteers of different age and gender (to just name two demographic variables). In particular, age is known to have a severe effect on heart motion. Ideally, one would compare a patient dataset only against healthy volunteers of the same demographic group, which presumably would lead to much more accurate results. Still, we were able to show that our visual analysis methods can be effective and intuitive.

Another factor that was a challenge for us was the missing heart rate information, e.g., acquired using an electrocardiogram. Such information would allow us to better synchronize the data. In fact, when generating the FBPs for the healthy cohort, some healthy volunteers turned out to be outliers for some segments, which we excluded then from the cohort. Further inspection showed that an imprecise synchronization most likely caused the healthy volunteer to be an outlier.

Computing outliers is a helpful method for detecting potential pathologies. However, there are many segments (such as segment 7 in Figure 8c), where there are severe differences to the cohort without being detected as an outlier. This documents that relying just on automatic methods does not suffice and that our visual analysis workflow can improve the analysis. On the other hand, we observed that healthy volunteers also exhibit differences to the 100% band as shown in Figure 8a. As one of the volunteers must have the maximum value in each time point among the cohort, such differences must exist. These differences are small, but they still caused some confusion in our user study. We believe that users would be in a better position to interpret these cases after having seen a few of them, as TPM is not yet clinical routine.

In terms of future directions, we would like to look into other derived indicators such as time-to-peak (TTP) for velocities, dyssynchrony calculations, or temporal changes in wall thickness, and

we would like to build cohorts of patients with certain types of anomalies such as hypokinetic, akinetic, or dyskinetic and analyze the difference between patient cohorts (also in comparison to the healthy cohort). We would also like to apply our visual encodings to other MR imaging methods such as myocardial perfusion, segmental strain analysis, late gadolinium enhancement (LGE), and extracellular volume (ECV) .

8. Conclusion

The comprehension of the spatio-temporal patterns and identification of anomalies in the myocardial motion are extremely challenging tasks. Our approach uses the concept of functional box plots to visualize the variability within a cohort, puts it into a layout for spatio-temporal analyses, and visually encodes locations and severeness of anomalies in an individual dataset by comparing it to the cohort. An analytical workflow with suitable visual encodings for different analytical steps was proposed and evaluated with medical experts.

References

[Cer02] CERQUEIRA M. D.: Standardized Myocardial Segmentation and Nomenclature for Tomographic Imaging of the Heart: A Statement for Healthcare Professionals From the Cardiac Imaging Committee of the Council on Clinical Cardiology of the American Heart Association. *Circulation 105*, 4 (Jan. 2002), 539–542. 2

[CHCM02] CLARYSSE P., HAN M., CROISILLE P., MAGNIN I. E.: Exploratory analysis of the spatio-temporal deformation of the myocardium during systole from tagged MRI. *IEEE Transactions on Biomedical Engineering 49*, 11 (2002), 1328–1339. 2

[CHS*16] CHITIBOI T., HENNEMUTH A., SCHNELL S., CHOWDHARY V., HONARMAND A., MARKL M., LINSEN L., HAHN H.: Contour tracking and probabilistic segmentation of tissue phase mapping mri. In *SPIE Medical Imaging* (2016), International Society for Optics and Photonics, pp. 978404–978404. 3

[CNS*15] CHITIBOI T., NEUGEBAUER M., SCHNELL S., MARKL M., LINSEN L.: 3d superquadric glyphs for visualizing myocardial motion. In *Poster Proceedings of 2015 IEEE Scientific Visualization Conference, SciVis 2015* (2015), pp. 143–144. 3

[CPS*15] CODREANU I., PEGG T. J., SELVANAYAGAM J. B., JUNG B. A., TAGGART D. P., ROTARU N.: Comprehensive Assessment of Left Ventricular Wall Motion Abnormalities in Coronary Artery Disease Using Cardiac Magnetic Resonance. *Journal of Cardiology and Neurocardiovascular Diseases 2*, 006 (2015). 2

[DAS*14] DUNCAN A. E., ALFIREVIC A., SESSLER D. I., POPOVIC Z. B., THOMAS J. D.: Perioperative assessment of myocardial deformation. *Anesthesia and analgesia 118*, 3 (2014), 525. 1

[FJG*11] FÖLL D., JUNG B., GERMANN E., HENNIG J., BODE C., MARKL M.: Magnetic resonance tissue phase mapping: Analysis of age-related and pathologically altered left ventricular radial and long-axis dyssynchrony. *Journal of Magnetic Resonance Imaging 34*, 3 (2011), 518–525. 8

[FJS*09] FÖLL D., JUNG B., STAEHLE F., SCHILLI E., BODE C., HENNIG J., MARKL M.: Visualization of multidirectional regional left ventricular dynamics by high-temporal-resolution tissue phase mapping. *Journal of magnetic resonance imaging : JMRI 29*, 5 (may 2009), 1043–52. 1, 2

[GBGCP08] GARCIA-BARNES J., GIL D., CARRERAS F., PUJADAS S.: Regional motion patterns for the left ventricle function assessment. In *Pattern Recognition, 2008. ICPR 2008. 19th International Conference on* (2008), IEEE, pp. 1–4. 2

[HB03] HARROWER M., BREWER C. A.: Colorbrewer. org: an online tool for selecting colour schemes for maps. *The Cartographic Journal 40*, 1 (2003), 27–37. 4

[HS10] HYNDMAN R. J., SHANG H. L.: Rainbow plots, bagplots, and boxplots for functional data. *Journal of Computational and Graphical Statistics 19*, 1 (2010), 29–45. 4

[JFB*06] JUNG B., FÖLL D., BÖTTLER P., PETERSEN S., HENNIG J., MARKL M.: Detailed analysis of myocardial motion in volunteers and patients using high-temporal-resolution mr tissue phase mapping. *Journal of Magnetic Resonance Imaging 24*, 5 (2006), 1033–1039. 2, 3

[LCB*16] LIN K., CHOWDHARY V., BENZULY K. H., YANCY C. W., LOMASNEY J. W., RIGOLIN V. H., ANDERSON A. S., WILCOX J., CARR J., MARKL M.: Reproducibility and observer variability of tissue phase mapping for the quantification of regional myocardial velocities. *The international journal of cardiovascular imaging 32*, 8 (2016), 1227–1234. 3

[LPS*99] LIU R. Y., PARELIUS J. M., SINGH K., ET AL.: Multivariate analysis by data depth: descriptive statistics, graphics and inference,(with discussion and a rejoinder by Liu and Singh). *The annals of statistics 27*, 3 (1999), 783–858. 4

[MRG*13] MARKL M., RUSTOGI R., GALIZIA M., GOYAL A., COLLINS J., USMAN A., JUNG B., FOELL D., CARR J.: Myocardial t2-mapping and velocity mapping: Changes in regional left ventricular structure and function after heart transplantation. *Magnetic resonance in medicine 70*, 2 (2013), 517–526. 1, 3

[PBI*13] PUNITHAKUMAR K., BEN AYED I., ISLAM A., GOELA A., ROSS I. G., CHONG J., LI S.: Regional heart motion abnormality detection: An information theoretic approach. *Medical Image Analysis 17*, 3 (2013), 311–324. 2

[PSY*94] PELC L. R., SAYRE J., YUN K., CASTRO L. J., HERFKENS R. J., PELC N. J., ET AL.: Evaluation of myocardial motion tracking with cine-phase contrast magnetic resonance imaging. *Investigative radiology 29*, 12 (1994), 1038–1042. 2

[RKL*07] REDHEUIL A. B., KACHENOURA N., LAPORTE R., AZARINE A., LYON X., JOLIVET O., FROUIN F., MOUSSEAUX E.: Interobserver variability in assessing segmental function can be reduced by combining visual analysis of cmr cine sequences with corresponding parametric images of myocardial contraction. *Journal of Cardiovascular Magnetic Resonance 9*, 6 (2007), 863–872. 2

[SCK*16] SHEHARYAR A., CHITIBOI T., KELLER E., RAHMAN O., SCHNELL S., MARKL M., BOUHALI O., LINSEN L.: Spatio-temporal Visualization of Regional Myocardial Velocities. In *Eurographics Workshop on Visual Computing for Biology and Medicine* (2016), The Eurographics Association. 2, 4, 5

[SFK*09] SUINESIAPUTRA A., FRANGI A. F., KAANDORP T. A. M., LAMB H. J., BAX J. J., REIBER J. H. C., LELIEVELDT B. P. F.: Automated Detection of Regional Wall Motion Abnormalities Based on a Statistical Model Applied to Multislice Short-Axis Cardiac MR Images. *Work 28*, 4 (2009), 595–607. 2

[SG11] SUN Y., GENTON M. G.: Functional boxplots. *Journal of Computational and Graphical Statistics 20*, 2 (2011), 316–334. 4, 5

[TBB*08] TERMEER M., BESCÓS J. O., BREEUWER M., VILANOVA A., GERRITSEN F., GRÖLLER M. E., NAGEL E.: Visualization of myocardial perfusion derived from coronary anatomy. *IEEE transactions on visualization and computer graphics 14*, 6 (2008), 1595–1602. 4

[TH13] TAIMOURI V., HUA J.: Visualization of shape motions in shape space. *IEEE transactions on visualization and computer graphics 19*, 12 (2013), 2644–2652. 2

[WN09] WANG J., NAGUEH S. F.: Current perspectives on cardiac function in patients with diastolic heart failure. *Circulation 119*, 8 (2009), 1146–1157. 1

[ZPR*88] ZERHOUNI E. A., PARISH D. M., ROGERS W. J., YANG A., SHAPIRO E. P.: Human heart: tagging with mr imaging–a method for noninvasive assessment of myocardial motion. *Radiology 169*, 1 (1988), 59–63. 3